Clinical Nutrition 38 (2019) 2349–2359

Contents lists available at ScienceDirect

Clinical Nutrition

journal homepage: http://www.elsevier.com/locate/clnu

Original article

Transcriptomics and proteomics analyses of anti-cancer mechanisms of TR35—An active fraction from Xinjiang Bactrian camel milk in esophageal carcinoma cell

Jie Yang [a], Zhihua Dou [a], Xi Peng [b], Hongjuan Wang [a], Tong Shen [a], Jun Liu [a], Guan Li [a], Yang Gao [b, *]

[a] Department of Bioengineering, College of Life Science and Technology, Xinjiang University, Urumqi, China
[b] School of Medicine, Nankai University, Tianjin, China

ARTICLE INFO

Article history:
Received 13 April 2018
Accepted 18 October 2018

Keywords:
Transcriptomics
Proteomics
Anti-cancer
Camel milk
Esophageal carcinoma

SUMMARY

Background & aims: The aim of the paper is to investigate the effect of the active fraction extracted from the Xinjiang Bactrian camel whey on the human cancer cells using an in vitro and in vivo model of human carcinoma of the esophagus.

Methods and results: Our results demonstrated that an antitumor active fraction, TR35, isolated from Xinjiang Bactrian camel milk could significantly inhibit Eca109 cell proliferation and induce its apoptosis (indicated by MTT assay, Annexin V-FITC Apoptosis Detection, and caspase-3 activity). Moreover, we found that TR35 could inhibit the growth of xenografted tumor in nude mice without loss in body weight. Furthermore, we used RNA-Seq and 2-DE combined Mass Spectrometry analysis to identify differentially expressed RNA and protein markers of apoptosis and necrosis. Compared with untreated Eca109 cells, a total of 405 differentially expressed genes and 55 differentially expressed proteins were identified in TR35 treated Eca109 cells. KEGG analysis uncovered signaling pathways closely associated with cancer inhibition that were enriched in the TR35-treated cells.

Conclusions: These results might implicate that downregulation of specific proteins identified in this study may be the cause of this tumor growth inhibition. This study sheds light on the potential therapeutic advantages based on the historical anti-cancer activities of camel milk.

1. Introduction

Esophageal cancer is currently the eighth most common malignancy and the sixth leading cause of cancer-related death worldwide [1]. Epidemiology of esophageal cancer is characterized by marked differences in prevalence between countries/regions/ethnic groups. For instance, it is rare in Western countries but is relatively prevalent in Asia, Southern and Eastern Africa, and northwestern France [2]. The highest incidence in the world is observed in populations of northwestern Xinjiang, China, where age-adjusted mortality may reach 150 of 100,000 [3]. The esophageal squamous cell carcinoma (ESCC) and esophageal adenocarcinoma (EAC) are two primary histological types of esophageal cancer. The differences in etiological and pathological characteristics. In high-incidence regions, ESCC is the dominant type [4]. Current therapeutics for esophageal cancer are mainly chemotherapy-based, and the overall 5-year survival for patients with ESCC remains less than 15% [5]. This highlights the necessity to identify preventive measures and alternative treatments for ESCC.

Certain dietary constituents have been demonstrated to play a beneficial role in health promotion in terms of chemoprevention. Dietary modulation has also emerged as a novel approach to control certain cancers [6]. Camel milk has been recognized for its extraordinary medicinal properties. It has beneficial effects on diabetes [7], hepatitis [8], allergy [9], lactose intolerance [10], autism [11] and alcohol-induced liver damage [12]. The regional pharmacopoeia from Xinjiang, Uygur, claimed that camel milk as a traditional food may counter the effects of serious diseases and treat cancers including ESCC. However, this claim has not yet been thoroughly studied.

* Corresponding author. School of Medicine, Nankai University, 94 Weijin Road, 217 Room, Tianjin 300071, China. Fax: +86 22 23504334.
E-mail address: Gaoy@nankai.edu.cn (Y. Gao).

https://doi.org/10.1016/j.clnu.2018.10.013

Until now, only a handful of reports have been published regarding anticancer properties of camel milk [13–15]. In the present study, we isolated a mixture fraction, TR35, from Xinjiang Bactrian camel milk. And evaluated the potential effect of TR35 on Eca-109 esophageal cancer cells, in vitro and in vivo. We show that TR35 induces apoptosis of Eca-109 and limits tumor progression. Transcriptomic and proteomic analysis were harnessed to further explore the underlying molecular mechanism of cell death in the Eca-109 cells.

2. Materials and methods

2.1. Materials

The active fraction named TR35 was extracted from Xinjiang Bactrian camel whey and the M35 fraction was extracted from bovine whey with the same methods in our laboratory (Supplementary Materials and methods 1).

2.2. Cells

The human esophageal cancer cell line, Eca109 was obtained from the Cell Bank of Shanghai. Cells were cultured in RPMI 1640 medium containing 10% heated inactivated fetal bovine serum (FBS, Gibco, USA) and 100 units/ml penicillin/streptomycin. Cells were kept in an incubator at 5% CO_2 and 37 °C.

2.3. Cell viability by MTT assay

The cytotoxic effect of TR35 and M35 on Eca109 cells was evaluated by MTT assay. Eca109 cells were seeded in 96-well plates at a density of 10^4 cells per well, and incubated overnight to allow cell attachment. TR35 was dissolved in the culture medium and administered to the cells at 0 mg/ml, 0.5 mg/ml, 1 mg/ml, 2 mg/ml, 4 mg/ml and 8 mg/ml, 5-fluorouracil 20 μg/ml was used as a positive control, 1 mg/ml, 2 mg/ml, 4 mg/ml M35 (also dissolved in the culture medium) were used as negative control. After incubation for 0 h, 24 h, 48 h, or 72 h, MTT (20 μl) was added to each well and incubated for 4 h at 37 °C. An aliquot of 150 μl of DMSO was added to dissolve formazan crystals. The plates were shaken for 10 min, and absorbance of formazan crystals was measured at 490 nm. Experiments were performed in triplicate. Suppression ratio was calculated as the percentage of MTT inhibition using the following equation: suppression ratio = (1 − mean experimental absorbance/mean control absorbance) × 100%.

2.4. Cell apoptosis assay

Eca109 cells (1×10^6 cells/well) were seeded in 6-well plates and incubated overnight to allow cell attachment. After treatment with TR35 at 0 mg/ml, 1 mg/ml, 2 mg/ml and 4 mg/ml for 48 h, cells were washed three times with PBS. Samples were prepared following manufacturer's instructions using the Annexin V-FITC Apoptosis Detection Kit (Univ, China). Prepared cells were analyzed on the Epics Altra II flow cytometer (Beckman Coulter, USA). Apoptosis rate was calculated by averaging the number of early and late apoptotic cells. Experiments were performed in triplicate.

2.5. Nuclear morphology study by Hoechst 33258

To observe nuclear changes during apoptosis, the chromatin-specific dye Hoechst 33258 was applied to Eca109 cells (1×10^6 cells/well) in 6-well plates. After 48-hour incubation with 4 mg/ml TR35, cells were stained with Hoechst dye (10 μg/ml) for 30 min and washed with PBS. The cells were analyzed under a fluorescence microscope (Nikon, Tokyo, Japan) and photographed.

2.6. Caspase-3 activity

Caspase-3 activity was assayed using the eBioscience ELISA Assay kit following the manufacturer's instructions. Cells were seeded in 75 cm^2 flasks at a density of 5×10^6 cells/flask. After administration of TR35 at 0 mg/ml, 1 mg/ml, 2 mg/ml and 4 mg/ml for 48 h, cells were harvested and washed with PBS. Collected cells were incubated with lysis buffer at room temperature for 60 min and centrifuged at $1000 \times g$ for 15 min. Subsequent steps were performed following manufacturer's protocol and absorbance was measured at 450 nm.

2.7. RNA-seq analysis

Eca109 cells were seeded in two 75 cm^2 flasks at a density of 5×10^6 cells/flask. One flask was treated with TR35 (4 mg/ml), while the other was untreated (control). Total RNA was isolated using the High Pure RNA Isolation Kit (Roche) after 48-hour incubation. cDNA Library preparation was done using the RNA-Seq Sample Prep Kit (Illumina) according to the manufacturer's instructions. For the QC step, Agilent 2100 Bioanalyzer and ABI StepOnePlus Real-Time PCR System were used to qualify and quantify of the sample library. Each cDNA library was sequenced by Beijing Genomics Institute (BGI, Shenzhen, China) via HiSeq 2000 (Illumina).

2.8. Protein extraction and 2-DE analysis

Eca109 cells were seeded in two 75 cm^2 flasks at a density of 5×10^6 cells/flask. One flask was treated with TR35 (4 mg/ml), while the other was untreated (control). After 48 h, cells were harvested, washed, and 1 ml of lysis buffer (7M urea, 2M thiourea, 4% CHAPS, 2 mM TBP, IPG buffer 3-10NL, and protease inhibitor cocktail) was added to each tube. After incubation with lysis buffer for 30 min at 4 °C, whole cell lysates were collected after centrifugation ($15000 \times g$) for 30 min at 4 °C. Cellular lysates were purified using the 2-D Clean-Up Kit (GE Healthcare) and quantified using Bio-Rad protein assay (Bio-Rad). Three replicates were used for 2-D Electrophoresis. 2-DE and Image Analysis was performed as outlined by Gao et al. (2009). (briefly described in Supplementary Materials and methods 2).

2.9. Protein identification by MALDI-TOF mass spectrometry

Spots were excised in an automated ProPic station (Genomic Solutions, Bath, UK). After excision from the 2D gel, protein spots were digested following in-gel digestion protocol [16]. Digested samples were then prepared for MALDI-TOF/TOF analysis. Digested peptides were analyzed using the 4800 MALDI-TOF/TOF Proteomics Analyser (Applied Biosystems, Foster City, CA, USA). MS analysis and database searching were performed as described by Gao et al. (2009). (briefly described in supplementary Materials and methods 2).

2.10. Animals and treatment

Ten BALB/c nude mice (4 weeks old, weighing 20–24 g) were obtained from Beijing Vital River Laboratory Animal Technology Co., Ltd. (Beijing, China), and maintained in animal house in school of life science of Nankai University. All animal experimental protocol used in this study was approved by the Institutional Animal Care and Use Committee of the Nankai University (20170003) and complied with the National Institutes of Health guide for the care

and use of Laboratory animals (NIH Publications No. 8023, revised 1978) The mice were housed under specific pathogen-free conditions with constant temperature (23 ± 2 °C) and controlled light (12 h light:12 h dark). Ten mice were divided into two groups randomly (5 nude mice/group). Treated group were given TR35 (4 mg/ml, dissolved in Milli-Q water) 1 ml by gavage and control group were given same volume of water instead, Twice a day. Two weeks later, each nude mice was injected subcutaneously with 2×10^6 Eca-109 cells on the back side by axillary.

2.11. Measurement of body weight and tumor sizes

Body weight was measured every five days. After the appearance of subcutaneous scleroma, the long diameter (A) and short diameter (B) were measured every seven days. The tumor volume was calculated using the formula: Volume = 0.5 length × width^2. After the nude mice were executed, the tumors were completely harvested and weighted.

2.12. Protein identification of TR35 and M35

200 μg of proteins for each sample (TR35 and M35) were incorporated into 30 μl SDT buffer (4% SDS, 100 mM DTT, 150 mM Tris–HCl pH 8.0). Then proteins were digested following filter-aided sample preparation (FASP Digestion) protocol. Digested samples were then prepared for nanoLC-MS/MS analysis. Digested peptides were analyzed using the Q Exactive mass spectrometer (Thermo Scientific, USA) that was coupled to Easy nLC (Proxeon Biosystems, now Thermo Fisher Scientific, USA). MS/MS spectra were searched using MASCOT engine (Matrix Science, London, UK; version 2.2). All the details of this identification process were described in supplementary Materials and methods 3.

2.13. Statistical analysis

All data are presented as means of at least three different experiments ± standard deviation (SD). Student's t-test was used to compare the results. A p value < 0.05 was considered statistically significant.

3. Results

3.1. TR35 reduces proliferation of Eca109 cells

MTT Assay. To determine whether TR35 inhibits cancer cell growth and proliferation, Eca109 cells were treated for 24, 48 and 72 h with increasing concentrations of TR35 (0.5, 1, 2, 4, and 8 mg/ml). Cells incubated with 5-fluorouracil (20 μg/ml) were used as a positive control. Proliferation status of Eca109 cells were monitored by absorbance at 490 nm. Figure 1A demonstrates that treatment of Eca109 cells with TR35 resulted in a concentration and time-dependent suppression of cell growth and proliferation. This result was reflected in cell survival rate, and a strong negative effect on proliferation was observed at a TR35 concentration of 4 mg/ml (Fig. 1A).

To test whether M35 from bovine whey had the same function with TR35, Eca109 cells were also treated with M35 (1, 2, 4 mg/ml) for 24, 48 and 72 h. Compared with 90% suppression ratio of 4 mg/ml TR35, the highest suppression ratio of M35 is only 28% (Fig. 1A).

3.2. TR35 induces apoptosis in Eca109 cells

Cell apoptosis assay. A previous study demonstrated that camel's milk could induce apoptosis in Hepatoma and breast cancer cell lines [17]. Therefore, we attempted to use the Annexin V-FITC/PI assay to determine if the inhibition of cell proliferation of TR35 was due to apoptosis. As shown in Fig. 1B, treatment of Eca109 cells with a series of TR35 concentrations for 48 h led to a significant increase in the percentage of early or late apoptotic cells, and a significant decrease in the percentage of viable cells. Treatment of Eca109 cells with 4 mg/ml of TR35 for 48 h resulted in a decrease of 93.9%–43.0% viability, increase of 2.6%–28.3% in early apoptosis, and increase of 3.1%–35.4% in late apoptosis, relative to untreated controls.

Nuclear morphology imaging with Hoechst Stain. To study the effect of TR35 treatment on nuclear morphology, the nucleic acid stain Hoechst 33342 was applied to Eca109 cells in culture. After treatment with TR35 (4 mg/ml) for 24 h, fragmented nuclei were observed in TR35-treated cells (Fig. 1C). The results obtained from fluorescence microscopy indicated that TR35 treatment causes nuclear fragmentation in Eco109 cells.

Caspase-3 Activity. Figure 1D shows the effect of TR35 on caspase 3 activity. The increase of caspase 3 activity in cells treated with TR35 ($p < 0.01$) was statistically significant. As depicted in Fig. 1D, increase in caspase 3 activity occurred in a dose-dependent manner.

3.3. RNA-seq

Illumina sequencing and de novo assembly. In order to uncover the effect of TR35 on cancer cell growth, we sequenced two cDNA libraries taken from Eca109 cells treated with 4 mg/ml TR35 and without treatment for 48 h: 4mgA and conA, respectively. In the issue, we mapped the 23.9 million clean reads to the human genome, and assembled them into 16,718 genes. Total genes mapped from each sample were 15,983 (4mgA) and 15,915 (conA), respectively (Supplemental Table 1).

RNA-Seq global data analysis and evaluation of differential gene expression. RPKM (Reads per kb per million reads) method was used to calculate gene expression levels. Detailed expression profiles from the two samples are provided in Supplemental Table 2 (http://123.206.60.57/Portals/_default/Supplemental%20Table%202.xls?ver=2018-09-11-102037-510). To further determine gene expression changes between samples, we use DEG (differentially expressed genes) to describe fold change of the normalized (RPKM) expression values, and was at the fewest 2 in either direction when the |log2 ratio| ≥ 1 and FDR ≤ 0.001. Using an algorithm optimized by Mortazavi et al. [18], we identified 405 DEGs across two samples (4mgA-v-conA) (http://123.206.60.57/Portals/_default/Supplemental%20Table%203.xls?ver=2018-09-11-101848-290), which included 260 up-regulated genes and 145 down-regulated genes.

Functional annotation by KEGG. Of the 405 differentially expressed transcripts identified from the RPKM analysis, 341 genes belonged to 196 KEGG pathways. Twenty pathways were significantly different ($p < 0.05$) in response to TR35 treatment determined by hypergeometric distribution. Many signaling pathways closely associated with cancer cell development were suggested. For example: pathways in cancer (Table 1).

3.4. Proteomic level

Two Dimensional Analysis of Differentially Expressed Proteins. To study differential expression of proteins under the treatment of TR35, we used 2-D Electrophoresis to separate proteins from the Eca109 cells incubated with 4 mg/ml TR35 for 48 h, or those without treatment. For 2-DE, each sample (treated and untreated) was cultured in triplicate. From each biological replicate, proteins were separated on 2-D PAGE gel from whole-cell lysate. After Coomassie Brilliant Blue staining, over 2000 spots were detected on each 2-DE gel (Mw range: 10–200 kDa, *p*I range: 3–10NL) (Supplemental Fig. 1).

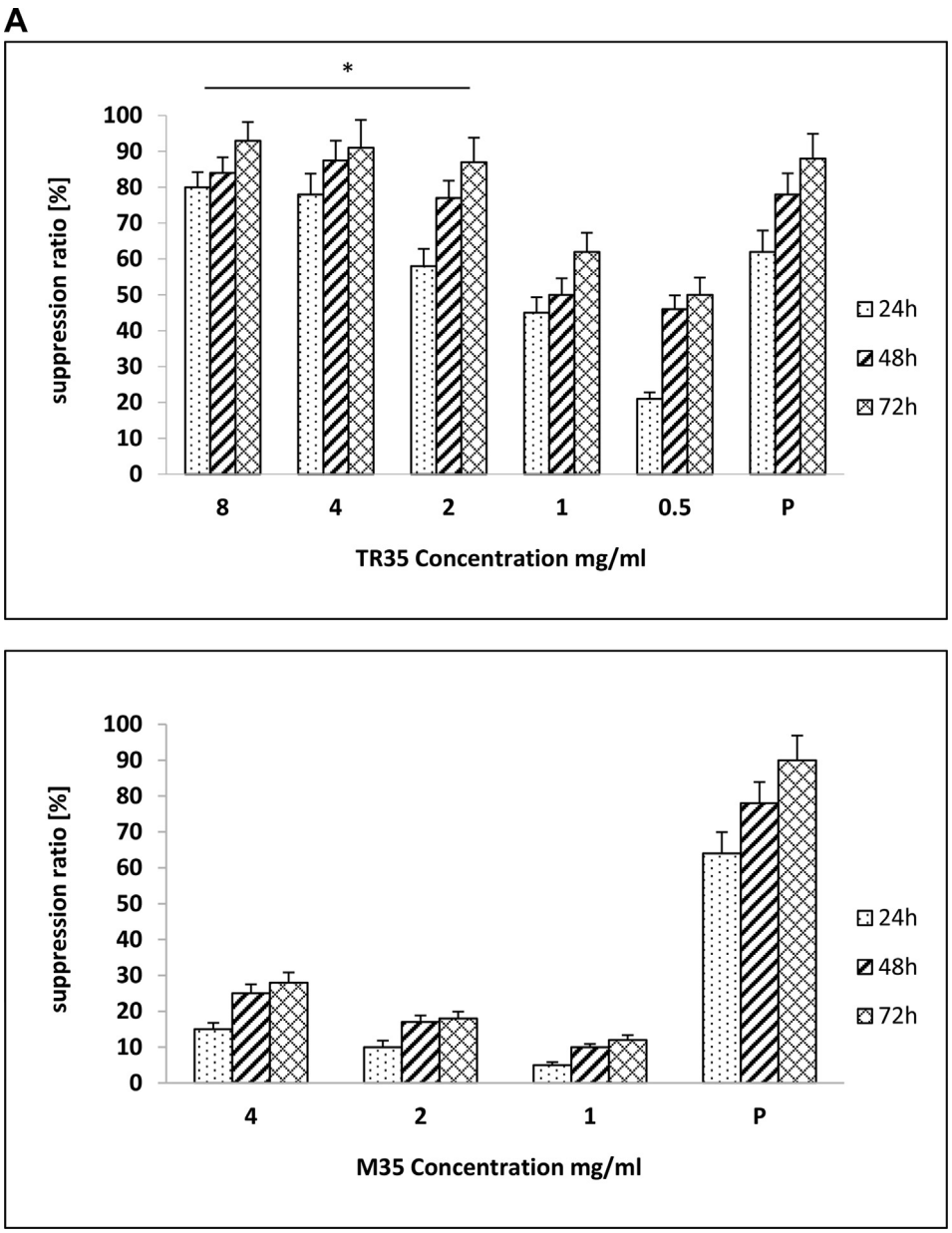

Fig. 1. Effects of TR35 on Eca-109 cells (A) Different concentration of TR35 and M35 inhibited the proliferation rate of Eca-109 cells (P: positive control). Suppression ratio was calculated as the percentage of MTT inhibition. Data are presented as the mean ± SD, n = 3. *p < 0.05. (B) Flow cytometry analyses were carried out to determine the early (the lower right quandrant) and late (the upper right quadrant) apoptosis rate of Eca-109 cells treated with different concentration of TR35. Data are presented as the mean ± SD, n = 3. *p < 0.05. (C) Hochest 33258 staining map of control group cells and TR35 treated cells. (D) Effect of different concentrations (0, 1, 2 and 4 mg/ml) of TR35 on Caspase-3 activity in Eca-109 cells after 24 h. The activity was determined using Caspase 3 assay kit following the manufacturer instructions. Data are presented as the mean ± SD, n = 3. **p < 0.01 versus control group.

Based on the statistical comparisons of spot-to-spot intensity, differentially expressed protein spots were defined as having 1.5-fold change between treated gels and the corresponding controls (p-value <0.05). A total of 55 protein spots had statistically significant differences in expression. This list was narrowed down to 33 protein spots with a fold-change difference greater than two. Eight of these were up-regulated, 14 were down-regulated, and 11 spots were almost absent in the treated cells compared to controls (Fig. 2A, B).

Correlation analysis of RNA and protein expressions. We compared the proteomic results with RNA-Seq global data to clarify the correlation of expression level in protein and mRNA. Sixteen of the 55 differentially expressed proteins showed the same fold-change (up or down) between protein and mRNA data (Table 2).

Correlation of differentially expressed proteins and their gene transcripts are only a small fraction (29%) in the TR35 treated Eca109 cells. This is common in such experiments and the reason may be posttranslational modifications, posttranscriptional regulation, or other unknown factors during experiment procedure.

3.5. Measurement of body weight and tumor sizes

After in vitro experiment, we examined the anti-tumor activity of TR35 in vivo. Eight days after the cells were injected with Eca-

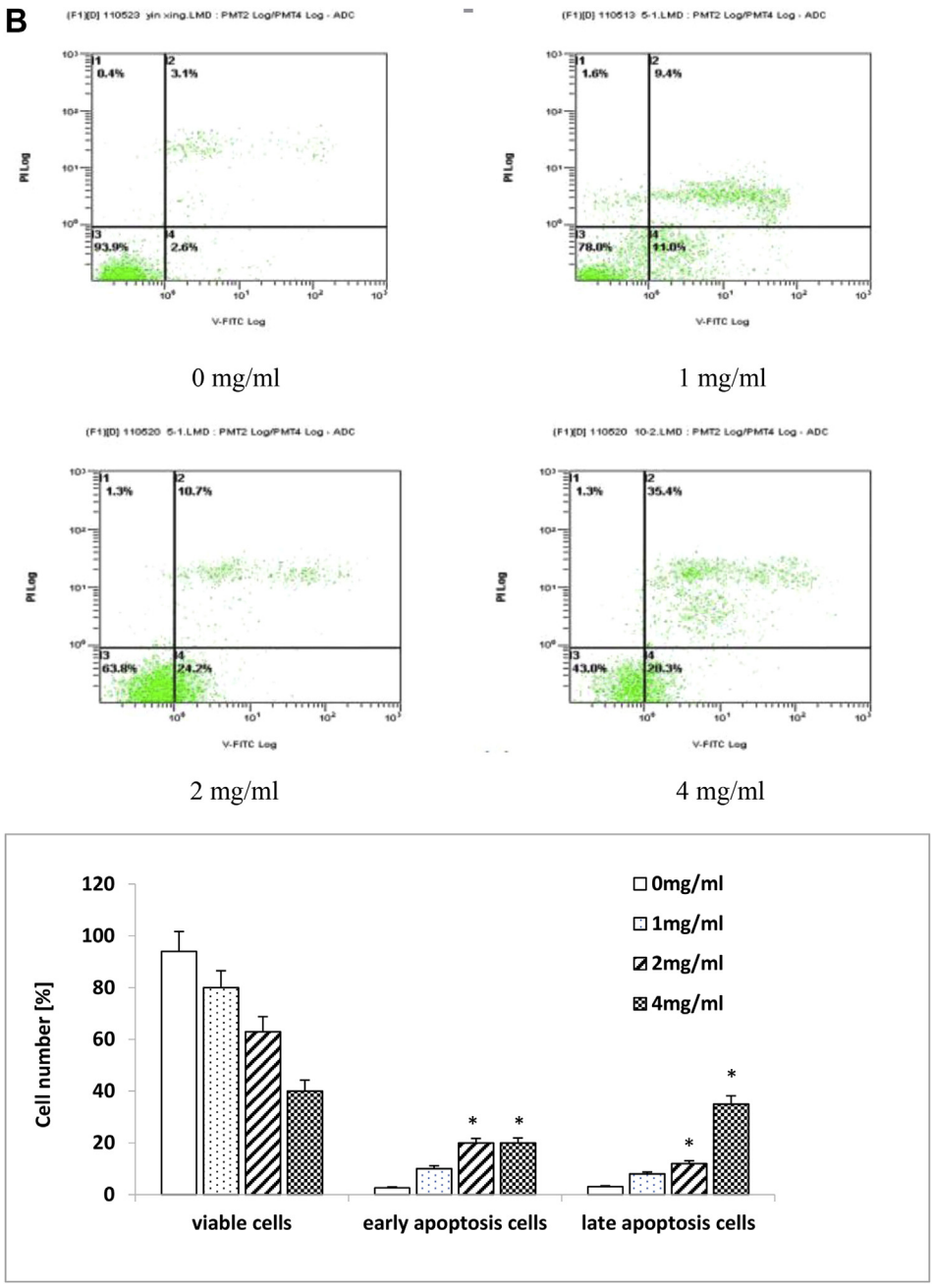

Fig. 1. (*continued*).

109, the transplanted tumors became visible with the naked eye, while much larger tumors were seen 20 days later. After 55 days of treatment, tumors were excised from each animal to determine tumor weight and assessment of the antitumor effect of TR35. Tumor weight and tumor volume in TR35-treated group were significantly smaller than that in control group (Fig. 3A, B, C). There was no significant change in the animal body weight following TR35 treatment (Fig. 3D).

3.6. Protein identification of TR35 and M35

A total of 14 different proteins were successfully identified by mass spectrometry after trypsin hydrolysis (Table 3). TR35 consisted of 13 proteins and M35 contained mixtures of 9 proteins. Eight of them were existed in both TR35 and M35, but the abundance varies widely. The four most abundant proteins in TR35 were Glycosylation-dependent cell adhesion molecule 1 (GlyCAM1, 42.8%), Alpha-lactalbumin (α-LA, 15.27%), Whey acidic protein (WAP, 13.36%), and Peptidoglycan recognition protein 1 (PGLYRP1, 12.68%). In M35, the three most abundant proteins were GlyCAM1 (81.02%), Polymeric immunoglobulin receptor (pIgR, 7.73%), and α-LA (7.23%). Each of the other six proteins in M35 accounted for less than two percent. The proteins only appeared in TR35 were WAP, Ig gamma-3 chain C, Ig lambda chain C, Beta-2-microglobulin (Beta(2) m) and one Uncharacterized protein. The protein levels of Neutrophil gelatinase-associated lipocalin-like protein and PGLYRP1 in TR35 is 150 times and about 23.5 times more than those of M35.

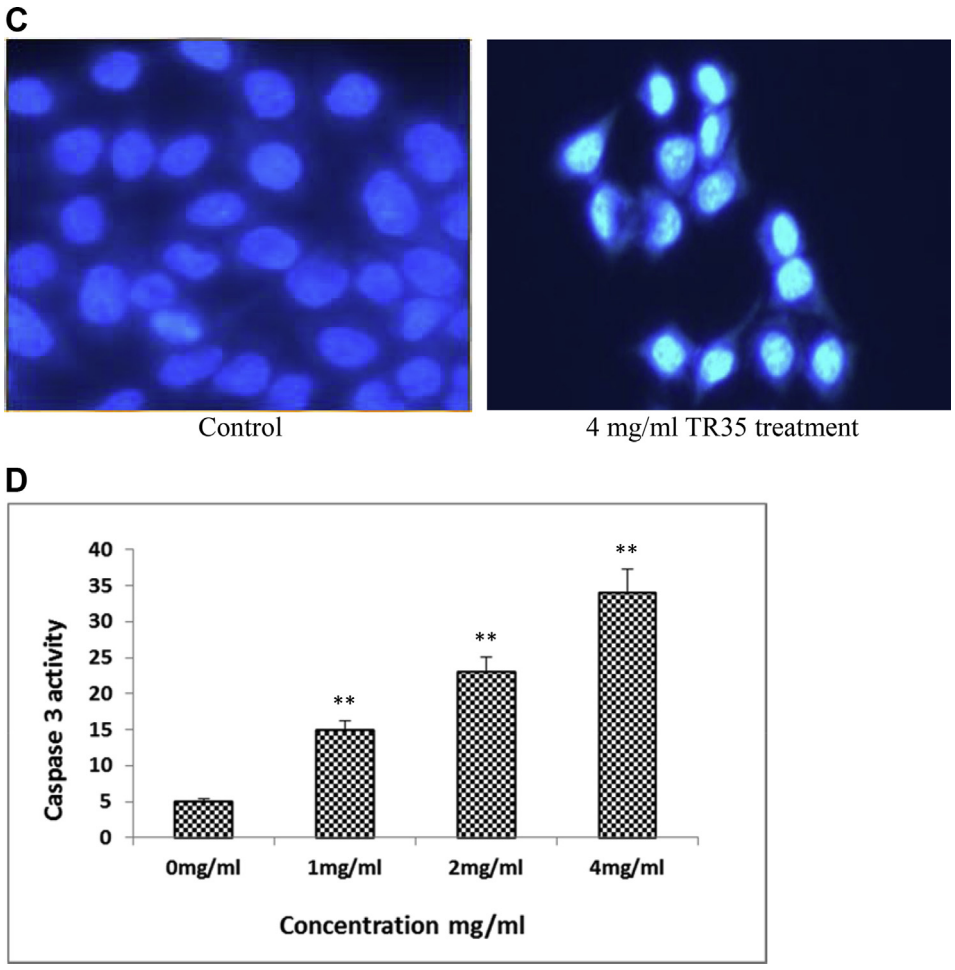

Fig. 1. (*continued*).

4. Discussion

Quality of life for patients with esophageal cancer are often seriously diminished due to the late diagnosis and esophageal obstruction. Current therapeutics for esophageal cancer still revolve around chemotherapy or radiotherapy. Novel therapies are urgently required for this form of cancer. Previous studies from our laboratory have found that TR35 effectively inhibits growth and proliferation of many human cancer cells, esophageal cancer, lung cancer and colon cancer (data not shown). However, the molecular mechanisms behind this phenomenon are still not clear.

This study reports on our initial investigations of the anti-proliferative effect of TR35 on the esophageal carcinoma Eca109 cell line and suppress growth of tumor xenograft in nude mice. We selected this cell line due to the high rates of esophageal cancer in Xinjiang province. Qualitative and quantitative data of this study suggest that this fraction inhibits proliferation of the Eca109 cells and induces cell death mainly via apoptosis. For instance, Hoechst staining revealed that the TR35 induced cytotoxic effect led to nuclear blebbing associated with apoptosis. This finding was confirmed by dose-dependent increase in AnnexinV binding to exposed phosphatidylserine on the cell surface. Previous work demonstrates that phosphatidylserine exposure may be initiated by caspase independent or dependent pathways [19]. Because caspase 3 activity is one of the key elements in activating the Xrp8 protein, which is responsible to translocation of phosphatidylserine to cell surface [20]. Our results suggested that TR35 might initiate phosphatidylserine exposure by a caspase 3-dependent pathway.

Apoptosis is a tightly regulated process under the control of several signaling pathways. As a deep investigation, molecular mechanisms of TR35-induced cell growth inhibition and apoptosis were further explored by RNA sequencing and proteomics using 2-D Electrophoresis. Taking advantage of this combined transcriptome and proteome analysis, we could supply an integrated interpretation and precise measurement of gene and protein expression within TR35 treated Eca109 cells.

From our cDNA library, 16692 transcripts were returned with different expression levels between the treated and untreated Eca109 cell samples. Using $|\log2\ \text{ratio}| \geq 2$ and FDR ≤ 0.001 as a filter, we obtained 65 genes including 34 upregulated and 31 downregulated genes. Seventeen upregulated genes were closely related to development of tumors. Within these 17 genes, 7 were associated with apoptosis, accounting for 41% of the total. Four genes: DDIT3, ASNS, NUPR1, and Chac1 may induce apoptosis through endoplasmic reticulum stress pathway. Previous work using nobiletin-treated calls suggested increased levels of DDIT3 and ASNS proteins will lead to apoptosis and suppressions of oxidative stress pathways and cell proliferation [21]. NUPR1 has been implicated as a key player in cellular stress response and is involved in metastasis of several cancers [22]. The depletion of viable candidates of DDIT3 and NUPR1 may possibly repress of ER stress [23]. *Chac1*-encoded proteins have been associated with the pro-apoptotic effect of unfolded protein response [24]. Activation of CHAC1 could increase calcium influxes and the induction of cell cycle arrest. Recently, Chac1 was identified as a novel pro-apoptotic factor in cells under ER stress [25].

Table 1
conA-VS-4mgA:KEGG pathway enrichment result.

#	Pathway	DEGs with pathway annotation (341)	All genes with pathway annotation (16502)	*p*-value	Pathway ID
1	Insulin signaling pathway	12 (3.52%)	242 (1.47%)	4.63E-03	ko04910
2	Renal cell carcinoma	7 (2.05%)	110 (0.67%)	7.84E-03	ko05211
3	MAPK signaling pathway	17 (4.99%)	430 (2.61%)	8.32E-03	ko04010
4	PPAR signaling pathway	8 (2.35%)	140 (0.85%)	8.67E-03	ko03320
5	Jak-STAT signaling pathway	10 (2.93%)	200 (1.21%)	8.84E-03	ko04630
6	Adipocytokine signaling pathway	7 (2.05%)	120 (0.73%)	1.23E-02	ko04920
7	Complement and coagulation cascades	9 (2.64%)	182 (1.1%)	1.35E-02	ko04610
8	Fc epsilon RI signaling pathway	8 (2.35%)	155 (0.94%)	1.53E-02	ko04664
9	Acute myeloid leukemia	6 (1.76%)	102 (0.62%)	1.92E-02	ko05221
10	Natural killer cell mediated cytotoxicity	10 (2.93%)	235 (1.42%)	2.46E-02	ko04650
11	Chagas disease (American trypanosomiasis)	7 (2.05%)	143 (0.87%)	2.92E-02	ko05142
12	B cell receptor signaling pathway	8 (2.35%)	176 (1.07%)	0.03	ko04662
13	Prion diseases	6 (1.76%)	114 (0.69%)	0.03	ko05020
14	Type II diabetes mellitus	5 (1.47%)	90 (0.55%)	0.04	ko04930
15	Colorectal cancer	5 (1.47%)	91 (0.55%)	0.04	ko05210
16	Pathways in cancer	18 (5.28%)	556 (3.37%)	0.04	ko05200
17	HTLV-I infection	13 (3.81%)	368 (2.23%)	0.04	ko05166
18	Toxoplasmosis	8 (2.35%)	189 (1.15%)	0.04	ko05145
19	Protein processing in endoplasmic reticulum	10 (2.93%)	262 (1.59%)	0.05	ko04141
20	mTOR signaling pathway	5 (1.47%)	96 (0.58%)	0.05	ko04150

DEGs: Different expression genes.

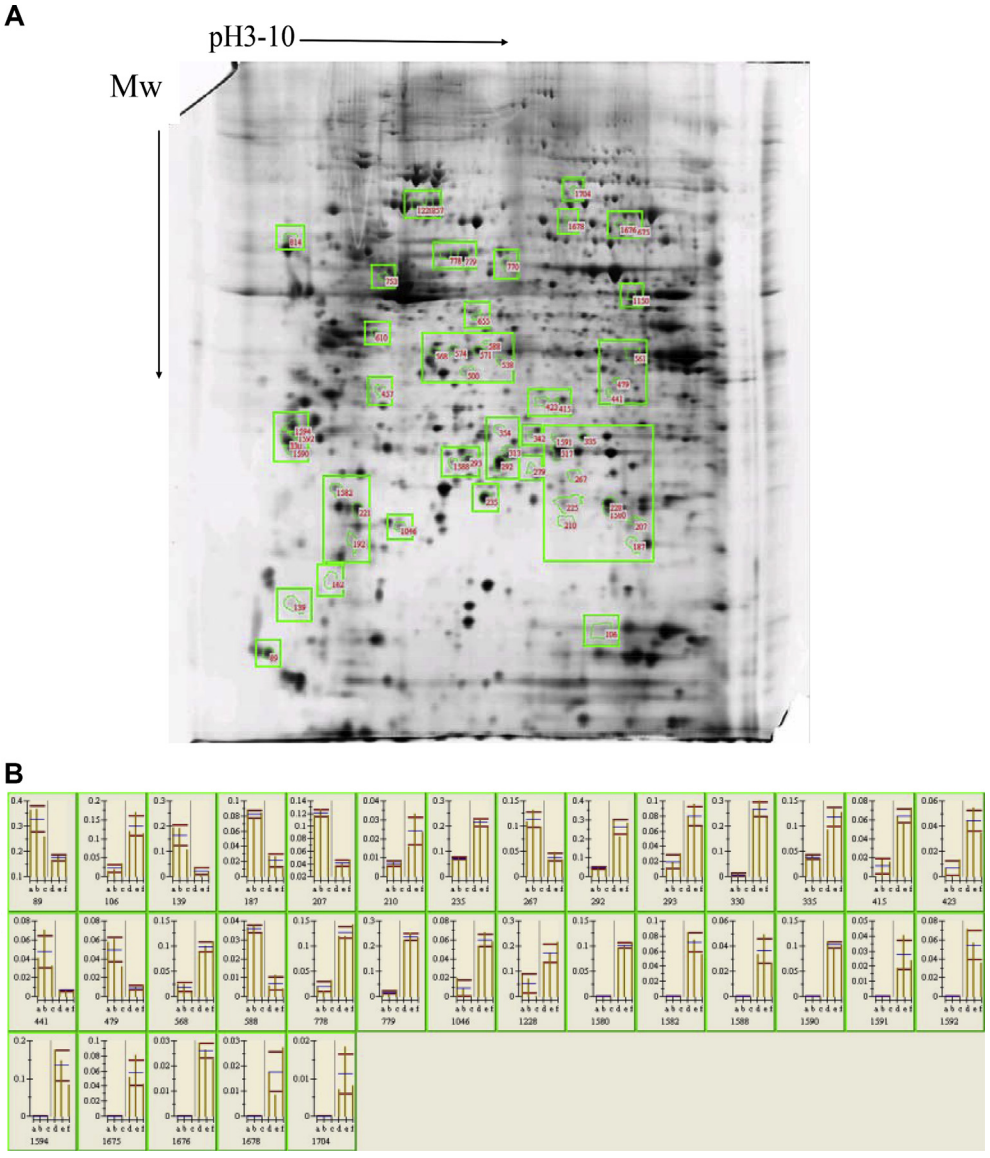

Fig. 2. (A) Proteome map of Eca-109 cells displaying all of the proteins that were found to be differently expressed with or without TR35 treatment. Spots with significant difference are indicated by numbers (B) Relative expression levels of 33 differently expressed proteins. Representative profiles from three independent experiments are shown.

Table 2
The consistent expression proteins at RNA and protein levels.

Swiss-prot Accession Number	Mw(kDa)/*p*I	Fold change in proteins	*p*-Value (proteins)	Mascot Score	Log_2 fold change in contigs	*p*-Value (contigs)	Protein annotation
gi|4505591	22.3/8.27	0.32	0.74E-02	104	−0.46	5.90E-57	peroxiredoxin-1/PRDX-1
gi|4501885	42/5.29	0.21	0.78E-02	141	−3.00	0.49	actin
gi|31543380	20/6.33	0.39	1.41E-02	574	−0.17	5.57E-03	protein DJ-1
gi|7661532	47/6.72	0.19	2.06E-06	55	−0.13	1.52E-02	RNA-binding protein NOB1
gi|20521876	26.4/8.3	0.37	0.35E-02	355	−0.33	1.578E-03	KIAA0081
gi|662841	22.4/7.83	0.25	0.05E-02	369	−0.96	1.42E-114	heat shock protein 27
gi|31542947	61.2/5.7	0.29	2.41E-02	978	−0.16	2.70E-06	60 kDa heat shock protein
gi|4506667	34.4/5.71	5.14	0.49E-02	415	0.18	8.80E-25	60S acidic ribosomal protein P0
gi|5031753	49.5/5.89	3.38	0.28E-02	491	0.17	1.91E-05	heterogeneous nuclear ribonucleoprotein H
gi|24234686	53.6/5.62	ND	2.85E-05	192	−1.50	1.78E-33	heat shock cognate 71 kDa protein isoform 2
gi|4505591	22.3/8.27	ND	2.55E-02	665	−0.46	5.90E-57	peroxiredoxin-1
gi|5771521	43.5/6.78	ND	0.03E-02	270	1.13	1.80E-283	3-phosphoglycerate dehydrogenase
gi|7657116	36.2/8.44	0.26	0.65E-02	607	−0.41	2.75E-08	glyceraldehyde-3-phosphate dehydrogenase
gi|4502601	31.2/7.7	3.69	0.33E-02	256	0.17	0.46	carbonyl reductase
gi|6912494	30.2/5.0	0.39	1.38E-02	140	−0.15	4.60E-03	microtubule-associated protein RP/EB family member 1
gi|4505701	35.3/5.7	0.27	0.56E-02	302	−0.26	3.94E-14	pyridoxal kinase
gi|5453595	51.9/8.07	ND	1.85E-07	191	−0.13	8.21E-03	adenylyl cyclase-associated protein 1

ND means the spot only appeared in control gels and were not detectable in treated gels.

Another factor not related to ER stress, ABCG1, is known to reduce intracellular and membrane-associated cholesterol levels, when its mRNA and protein level were increased. The deprivation of cholesterol from cancer cells has been revealed to inhibit cell proliferation, and on the other hand stimulate apoptosis [26].

RORα is also a potential tumor suppressor and inhibits tumor invasion by inducing suppressive cell microenvironment in breast cancer. Knock out of Rora weakened apoptotic cell death, whereas overexpression of Rora increased apoptosis [27]. In the process of some anticancer drugs treatment, for example nifurtimox or tamoxifen, caspase-3 activation and cancer cell apoptosis were observed and accompanied by up-regulation of SLC7A11 in a dose-dependent manner [28].

Other up-regulated tumor-related genes included IGFBP1, GDF-15, CYP26B1, SOCS2 and CASP14, which are shown as induced in different cancer treatment process. Triggering of these factors is suggested to prevent the development of cancer [29–31].

In 31 downregulated genes, fourteen were related to the development of tumors. Three of them (CKMT1A, Axin2 and HSPA2) were related to apoptosis, which accounts for about 21%. An

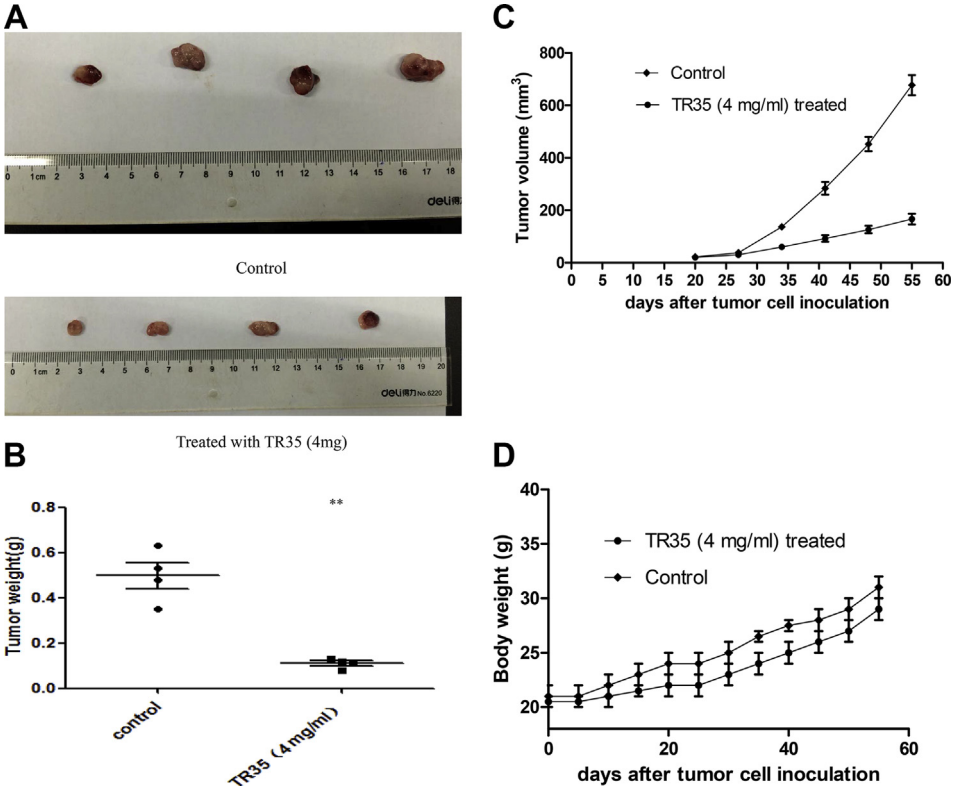

Fig. 3. Tumor inhibitory effect of TR35 in vivo. 2×10^6 Eca-109 cells/mouse were subcutaneously inoculated into nude mice. Ten mice were randomized into 2 groups (5 nude mice/group). One group treated with TR35 (4 mg) twice a days, another group with water at the same time for 55 days as previously mentioned. (A) The tumors were excised from animals after treatment. (B) The comparison of tumor weights of two groups. **P < 0.01 indicated significant differences compared with control group. (C) The tumor volumes were measured once every 7 days. Data are presented as the mean ± SD, n = 4. (D) The weight of mice was measured once every 5 days. Data are presented as the mean ± SD, n = 4.

Table 3
TR35 and M35 Component identification.

Protein Description (Fasta headers)	Number of proteins	Peptides	Unique peptides	Sequence coverage [%]	*Mol. weight [kDa]*	Percent in TR35	Percent in M35	Fold change (TR35/M35)
Glycosylation-dependent cell adhesion molecule 1	1	8	8	49.7	17.3	42.80	81.02	0.53
Alpha-lactalbumin	4	12	12	52.8	14.4	15.27	7.23	2.11
Whey acidic protein	3	6	6	76.1	12.6	13.36	0	∞
Peptidoglycan recognition protein 1	2	7	7	66.8	21.4	12.68	0.54	23.48
Uncharacterized protein 1	1	8	5	43.7	28.4	6.03	0.01	603
Ig gamma-3 chain C	1	11	8	38.8	37.6	3.99	0	∞
Ig lambda chain C	1	6	5	58.3	14.9	2.06	0	∞
Neutrophil gelatinase-associated lipocalin-like protein	1	9	9	42.1	28.4	1.50	0.01	150
Beta-2-microglobulin	1	4	4	43.2	13.7	0.67	0	∞
Uncharacterized protein 2	1	48	39	43.6	151.7	0.69	0.09	7.67
Lactoferrin	3	38	34	67.7	77.3	0.46	1.38	0.33
Uncharacterized protein 3	1	6	6	29	43.2	0.47	0	∞
Polymeric immunoglobulin receptor	2	20	3	45.7	82.4	0.02	7.73	0.003
Uncharacterized protein 4	2	8	8	34.1	51.7	0	1.99	0

siRNA-mediated reduced expression of CKMT1A led to increased cell apoptosis, and reduced proliferation, migration and invasion in HCC cell lines [32]. Compared with human normal oral keratinocytes, the expression level of Axin2, a potential oncogene, was much higher in KB oral cancer. Moreover, after Axin2 siRNA transfection, cell cytotoxicity and apoptotic population of KB oral cancer cells were largely increased [33]. HSPA2 can be expressed in human tumor cells at significant levels. Its downregulation induced apoptosis of HCC cells through the mitochondrial apoptotic pathway [34].

The results from RNA-Seq suggest a high likelihood that TR35 suppresses the Eca109 tumor cell growth through multiple pathways related to regulation of apoptosis or tumor development. When comparing proteomic and the transcriptomic levels for specific genes, only 29% of the differentially expressed proteins show correlation to their respective transcript level. This proves the difficulty of recapitulating protein expression of the mRNA transcript through paired proteomics and RNA-seq. Significantly, most changes to the proteome in TR35 treated Eca109 cells were a decrease to the individual protein levels (41/55). These lead to the conclusion that the mechanism underlying TR35-induced apoptosis may be via inhibition of transcription or translation of specific proteins related to cancer cell proliferation or survival. In this discussion, our focus are the genes and proteins with concomitant changes at mRNA and protein level. The genes which were only altered at translational level may be subject to further research.

Down-regulated proteins. The Heat Shock Proteins, including HSP60, HSPA8 and HSP27, were further investigated within our results due to their associated functions in apoptosis. Mitochondrion is the terminal usual pathway to apoptotic destruction. HSP60 is of upmost interest as it is a mitochondrial protein. Previous studies demonstrate a reduction of HSP60 in the cytoplasm leads to the releasing of “free” bax. Moreover, the number of bax raise significantly when HSP60 is downregulated, suggesting an immediate translocation of the unbound bax to mitochondria. The flux of bax to mitochondria have been suggested as sufficient to activate cytochrome c release and subsequent caspase activation [35].

Past proteomic analyses found HSPA8 was down-regulated in different cancer cell lines/types treated with chemotherapeutic agents. This downregulation was accompanied by suppression of cancer cell proliferation, migration, and invasion [36]. HSP27 inhibits apoptosis through the prevention of caspase 9 activation by cytochrome. This inhibition is perhaps a result of the binding of HSP27 to cytosolic cytochrome c. This inhibition may subsequently reduce apoptosome formation [37]. The binding of HSP27 to caspase 3 and caspase 3 probable modulation by HSP27 have also been documented [38]. Combined with RNA-Seq results, TR35 treatment depresses the expression of HSP family genes on both transcriptional and/or translational level (Supplemental Table 2). These findings might further elucidate anti-cancer mechanisms underlying the apoptotic effect of TR35.

It has been previously reported that DJ-1 (PARK7) can stimulates cell proliferation, cell invasion, and cancer metastasis, and HSP70 and Hsp27 were suggested to be closely involved in this Ras-dependent pathway [39].

PRDX1 might be attributed to the malignant transformation of NSCLC and esophageal cells. Comparing with paired normal tissues, expression of PRDX1 was significantly higher in ESCC tissues ($P < 0.05$) [40]. RNAi-mediated reduction of PRDX1 expression triggered cancer cell apoptosis through combined action of accumulation of ROS and enhancement of MAPK pathway activation [41].

NOB1 expression has previously been closely correlated with important histopathologic characteristics, recurrence, and metastasis of prostate carcinomas. When expression of NOB1 was inhibited by RNAi in vitro, proliferation and migration of many cancer cell types were suppressed and tumor apoptosis was induced [42]. The overexpression of CAP1 is connected with cancer cell migration and metastasis in esophageal squamous cell carcinoma [43]. The function of CAP1 in promoting tumor development has been suggested to be triggered, at least in part, by the modulation of CtBP2 and E-cadherin [44]. The down-regulation of other proteins included GAPDH, PHGDH, MAPRE1, PDXK and Actin, may enhance the apoptosis-inducing effects in some solid tumor cells [45–48].

Up-regulated proteins. For the remaining three overexpressed proteins (carbonyl reductase, 60S acidic ribosomal protein P0 and heterogeneous nuclear ribonucleoprotein H). The 5-year survival rate of carbonyl reductase (CBR)-high patients was 68.3%, significantly higher than that of CBR-low patients. Expression of CBR mRNA is a significant prognostic factor in non–small-cell lung cancer and is inversely associated with tumor progression and angiogenesis. The function of the other two proteins, 60S acidic ribosomal protein P0, and heterogeneous nuclear ribonucleoprotein H, remain unclear in ESCC. Together with KIAA0081, their role in esophageal cancer will need further exploration in follow-up studies.

By comparing the identification results of TR35 with M35, we found five proteins were only appeared in TR35 and the other five proteins level were much higher in TR35 than in M35. In these proteins, the anti-cancer and pro-apoptotic activity potential of α-LA [15], lactoferrin [13], WAP [49], and beta(2)m had been reported

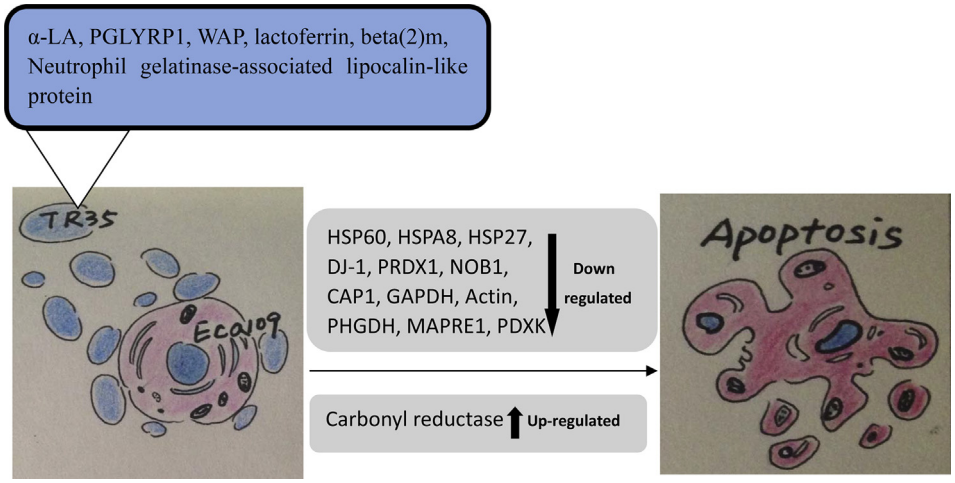

Fig. 4. The probable mechanism of the TR35 on the apoptosis events after the Eca-109 cell treatment. The upper gray box shows the proteins which are down-regulated by TR35 treatment. The lower gray box shows one protein which is up-regulated by TR35 treatment. These proteins were positively identified via the correlation of transcriptomics and proteomics results. The functions of these proteins were deeply tied to cell apoptosis.

[50]. The peptidoglycan recognition protein family member was shown to form a stable 1:1 complex with the major stress protein Hsp70. This complex induced apoptotic death in several tumor-derived cell lines even at subnanomolar concentrations [51]. Neutrophil gelatinase-associated lipocalin could induce apoptosis in human hepatocellular carcinoma cells through activation of mitochondria pathways [52]. The anti-cancer activities of TR35 was mainly depended on one special protein, or it was the result of synergistic action of multiple proteins, was our next research content.

In summary, this exploratory study provided a new knowledgebase for elucidating the molecular mechanisms of the anti-tumor activity of camel milk. After treatment with the active fraction, TR35, a total of 16 differentially expressed proteins were positively identified via the correlation of transcriptomics and proteomics results. The functions of these proteins were deeply tied to cell proliferation or apoptosis (Fig. 4). A few of the candidates will need further functional and clinical investigations. We must be aware the limitation of using a single cell culture system dictates caution in the interpretation of these results, and suggest that a conservative approach toward describing applications of TR35 as a novel cancer treatment is appropriate. Although camel milk has a beneficial action on liver [53], the toxicological aspects of TR35 still should be evaluated.

Funding

This work was supported by the National Natural Science Foundation of China (nos. 81101567 and 31260369).

Conflicts of interest

The authors declare that there are no conflicts of interest.

CRediT authorship contribution statement

Jie Yang: Conceptualization, Investigation, Formal analysis, Writing - original draft. **Zhihua Dou:** Data curation, Investigation. **Xi Peng:** Software, Writing - review & editing. **Hongjuan Wang:** Investigation. **Tong Shen:** Methodology. **Jun Liu:** Resources. **Guan Li:** Project administration, Supervision. **Yang Gao:** Conceptualization, Funding acquisition, Supervision, Writing - review & editing.

Appendix A. Supplementary data

Supplementary data to this article can be found online at https://doi.org/10.1016/j.clnu.2018.10.013.

References

[1] Kamangar F, Dores GM, Anderson WF. Patterns of cancer incidence, mortality, and prevalence across five continents: defining priorities to reduce cancer disparities in different geographic regions of the world. J Clin Oncol 2006;24:2137–50.
[2] Holmes RS, Vaughan TL. Epidemiology and pathogenesis of esophageal cancer. Semin Radiat Oncol 2007;17:2–9.
[3] Zheng ST, Vuitton L, Sheyhidin I, Vuitton DA, Zhang YM, Lu X. Northwestern China: a place to learn more on oesophageal cancer. Part one: behavioural and environmental risk factors. Eur J Gastroenterol Hepatol 2010;22:917–25.
[4] Fan YH, Yuan JM, Wang RW, Gao YT, Yu MC. Alcohol, tobacco, and diet in relation to esophageal cancer: the Shanghai Cohort Study. Nutr Cancer 2008;60:354–63.
[5] Lagergren J, Lagergren P. Oesophageal cancer. Brit Med J 2010;341(7784):1207–11.
[6] Kontou N, Psaltopoulou T, Panagiotakos D, Dimopoulos MA, Linos A. The mediterranean diet in cancer prevention: a review. J Med Food 2011;14:1065–78.
[7] Agrawal RP, Beniwal R, Kochar DK, Tuteja FC, Ghorui SK. Camel milk as an adjunct to insulin therapy improves long-term glycemic control and reduction in doses of insulin in patients with type-1 diabetes A 1 year randomized controlled trial. Diabetes Res Clin Pract 2005;68:176–7.
[8] El Miniawy HMF, Ahemad KA, Tony MA, Mansour SA, Khattab MMS. Camel milk inhibits murine hepatic carcinogenesis initiated by diethylnitrosamine and promoted by phenobarbitone. Indian J Vet Sci Med 2014;2:137–41.
[9] Shabo Y, Barzel R, Margoulis M, Yagil R. Camel milk for food allergies in children. Immunology and allergies. Isr Med Assoc J 2005;7:1–3.
[10] El-Agamy EI, Nawar M, Shamsia SM, Awad S, Haenlein GFW. Are camel milk proteins convenient to the nutrition of cow milk allergic children. Small Rumin Res 2009;82:1–6.
[11] Shabo Y, Yagil R. Etiology of autism and camel milk as therapy. Int J Disabil Hum Dev 2005;4:67–70.
[12] Ahmed AS, Abdalbagi NH, Mustafa HA, Idris AAA, Eltayb AMA, Ismail R. The role of camel milk in the reactivation of liver damaged by Sudanese liquor (Aragi). J Public Health 2011;6:157–63.
[13] Habib HM, Ibrahim WH, Schneider-Stock R, Hassan HM. Camel milk lactoferrin reduces the proliferation of colorectal cancer cells and exerts antioxidant and DNA damage inhibitory activities. Food Chem 2013;141(1):148–52.
[14] Badawy AA, El-Magd MA, AlSadrah SA. Therapeutic effect of camel milk and its exosomes on MCF7 cells in vitro and in vivo. Integr Cancer Ther 2018. https://doi.org/10.1177/1534735418786000. 1534735418786000.
[15] Uversky VN, El-Fakharany EM, Abu-Serie MM, Almehdar HA, Redwan EM. Divergent anticancer activity of free and formulated camel milk α-lactalbumin. Cancer Invest 2017;35(9):610–23.
[16] Gao Y, Xiong W, Li XB, Gao CF, Zhang YL, Li H, et al. Identification of the proteomic changes in Synechocystis sp. PCC 6803 following prolonged UV-B irradiation. J Exp Bot 2009;60:1141–54.

[17] Korashy HM, Maayah ZH, Abd-Allah AR, El-Kadi AO, Alhaider AA. Camel milk triggers apoptotic signaling pathways in human hepatoma HepG2 and breast cancer MCF7 cell lines through transcriptional mechanism. BioMed Res Int 2012;2012:593195.
[18] Mortazavi A, Williams BA, McCue K, Schaeffer L, Wold B. Mapping and quantifying mammalian transcriptomes by RNA-Seq. Nat Methods 2008 Jul;5(7):621–8.
[19] Ferraro-Peyret C, Quemeneur L, Flacher M, Revillard JP, Genestier L. Caspase-independent phosphatidylserine exposure during apoptosis of primary T lymphocytes. J Immunol 2002;169:4805–10.
[20] Mariño G, Kroemer G. Mechanisms of apoptotic phosphatidylserine exposure. Cell Res 2013;23:1247–8.
[21] Nemoto K, Ikeda A, Yoshida C, Kimura J, Mori J, Fujiwara H, et al. Characteristics of nobiletin-mediated alteration of gene expression in cultured cell lines. Biochem Biophys Res Commun 2013;431:530–4.
[22] Chowdhury UR, Samant RS, Fodstad O, Shevde LA. Emerging role of nuclear protein 1 (NUPR1) in cancer biology. Cancer Metastasis Rev 2009;28:225–32.
[23] Tang B, Li Q, Zhao XH, Wang HG, Li N, Fang Y, et al. Shiga toxins induce autophagic cell death in intestinal epithelial cells via the endoplasmic reticulum stress pathway. Autophagy 2015;11:344–54.
[24] Mungrue IN, Pagnon J, Kohannim O, Gargalovic PS, Lusis AJ. CHAC1/MGC4504 is a novel proapoptotic component of the unfolded protein response, downstream of the ATF4-ATF3-CHOP cascade. J Immunol 2009;182:466–76.
[25] Oh-Hashi K, Nomura Y, Shimada K, Koga H, Hirata Y, Kiuchi K. Transcriptional and post-translational regulation of mouse cation transport regulator homolog 1. Mol Cell Biochem 2013;380:97–106.
[26] Kim I, Xu W, Reed JC. Cell death and endoplasmic reticulum stress: disease relevance and therapeutic opportunities. Nat Rev Drug Discov 2008;7:1013–30.
[27] Xiong G, Wang C, Evers BM, Zhou BP, Xu R. RORalpha suppresses breast tumor invasion by inducing SEMA3F expression. Cancer Res 2012;72:1728–39.
[28] Koto KS, Lescault P, Brard L, Kim K, Singh RK, Bond J, et al. Antitumor activity of nifurtimox is enhanced with tetrathiomolybdate in medulloblastoma. Int J Oncol 2011;38:1329–41.
[29] Unsicker K, Spittau B, Krieglstein K. The multiple facets of the TGF-beta family cytokine growth/differentiation factor-15/macrophage inhibitory cytokine-1. Cytokine Growth Factor Rev 2013;24:373–84.
[30] Zhang P, Suidasari S, Hasegawa T, Yanaka N, Kato N. High concentrations of pyridoxal stimulate the expression of IGFBP1 in HepG2 cells through upregulation of the ERK/cJun pathway. Mol Med Rep 2013;8:973–8.
[31] Zhu JG, Dai QS, Han ZD, He HC, Mo RJ, Chen G, et al. Expression of SOCSs in human prostate cancer and their association in prognosis. Mol Cell Biochem 2013;381:51–9.
[32] Uranbileg B, Enooku K, Soroida Y, Ohkawa R, Kudo Y, Nakagawa H, et al. High ubiquitous mitochondrial creatine kinase expression in hepatocellular carcinoma denotes a poor prognosis with highly malignant potential. International journal of cancer. J Int Cancer 2014;134:2189–98.
[33] Kim JS, Park SY, Lee SA, Park MG, Yu SK, Lee MH, et al. MicroRNA-205 suppresses the oral carcinoma oncogenic activity via down-regulation of Axin-2 in KB human oral cancer cell. Mol Cell Biochem 2014;387:71–9.
[34] Xia LM, Tian DA, Zhang Q, Yan W, Wang B, Liu M, et al. Inhibition of HSP70-2 expression by RNA interference induces apoptosis of human hepatocellular carcinoma cells. Zhonghua gan zang bing za zhi = Zhonghua ganzangbing zazhi = Chinese Journal of Hepatology 2008;16:678–82.
[35] Kirchhoff SR, Gupta S, Knowlton AA. Cytosolic heat shock protein 60, apoptosis, and myocardial injury. Circulation 2002;105:2899–904.
[36] Matsuda Y, Ishiwata T, Yoshimura H, Hagio M, Arai T. Inhibition of nestin suppresses stem cell phenotype of glioblastomas through the alteration of post-translational modification of heat shock protein HSPA8/HSC71. Cancer Lett 2015;357:602–11.
[37] Bruey JM, Ducasse C, Bonniaud P, Ravagnan L, Susin SA, Diaz-Latoud C, et al. Hsp27 negatively regulates cell death by interacting with cytochrome c. Nat Cell Biol 2000;2:645–52.
[38] Pandey P, Farber R, Nakazawa A, Kumar S, Bharti A, Nalin C, et al. Hsp27 functions as a negative regulator of cytochrome c-dependent activation of procaspase-3. Oncogene 2000;19:1975–81.
[39] Shu KY, Xiao ZQ, Long SG, Yan JJ, Yu XH, Zhu QZ, et al. Expression of DJ-1 in endometrial cancer close correlation with clinicopathological features and apoptosis. Int J Gynecol Canc 2013;23:1029–35.
[40] Ren PF, Ye H, Dai LP, Liu M, Liu XX, Chai YR, et al. Peroxiredoxin 1 is a tumor-associated antigen in esophageal squamous cell carcinoma. Oncol Rep 2013;30:2297–303.
[41] He TT, Banach-Latapy A, Vernis L, Dardalhon M, Chanet R, Huang ME. Peroxiredoxin 1 knockdown potentiates beta-lapachone cytotoxicity through modulation of reactive oxygen species and mitogen-activated protein kinase signals. Carcinogenesis 2013;34:760–9.
[42] Li Y, Ma C, Qian M, Wen Z, Jing H, Qian D. Downregulation of NOB1 suppresses the proliferation and tumor growth of non-small cell lung cancer in vitro and in vivo. Oncol Rep 2014;31:1271–6.
[43] Li M, Yang X, Shi H, Ren H, Chen X, Zhang S, et al. Downregulated expression of the cyclase-associated protein 1 (CAP1) reduces migration in esophageal squamous cell carcinoma. Jpn J Clin Oncol 2013;43:856–64.
[44] Liu X, Yao N, Qian J, Huang H. High expression and prognostic role of CAP1 and CtBP2 in breast carcinoma: associated with E-cadherin and cell proliferation. Med Oncol 2014;31:878.
[45] Ganapathy-Kanniappan S, Kunjithapatham R, Torbenson MS, Rao PP, Carson KA, Buijs M, et al. Human hepatocellular carcinoma in a mouse model: assessment of tumor response to percutaneous ablation by using glyceraldehyde-3-phosphate dehydrogenase antagonists. Radiology 2012;262:834–45.
[46] Orimo T, Ojima H, Hiraoka N, Saito S, Kosuge T, Kakisaka T, et al. Proteomic profiling reveals the prognostic value of adenomatous polyposis coli-end-binding protein 1 in hepatocellular carcinoma. Hepatology 2008;48:1851–63.
[47] Bettayeb K, Sallam H, Ferandin Y, Popowycz F, Fournet G, Hassan M, et al. N-&-N, a new class of cell death-inducing kinase inhibitors derived from the purine roscovitine. Mol Canc Therapeut 2008;7:2713–24.
[48] Mashima T, Naito M, Tsuruo T. Caspase-mediated cleavage of cytoskeletal actin plays a positive role in the process of morphological apoptosis. Oncogene 1999;18:2423–30.
[49] Nukumi N, Iwamori T, Naito K, Tojo H. Whey acidic protein (WAP) depresses the proliferation of mouse (MMT) and human (MCF-7) mammary tumor cells. J Reprod Dev 2005;51(5):649–56.
[50] Min R, Li Z, Epstein J, Barlogie B, Yi Q. Beta(2)-microglobulin as a negative growth regulator of myeloma cells. Br J Haematol 2002;118(2):495–505.
[51] Yashin DV, Dukhanina EA, Kabanova OD, Romanova EA, Lukyanova TI, Tonevitskii AG, et al. The heat shock-binding protein (HspBP1) protects cells against the cytotoxic action of the Tag7-Hsp70 complex. J Biol Chem 2011 Mar 25;286(12):10258–64.
[52] Chien MH, Ying TH, Yang SF, Yu JK, Hsu CW, Hsieh SC, et al. Lipocalin-2 induces apoptosis in human hepatocellular carcinoma cells through activation of mitochondria pathways. Cell Biochem Biophys 2012;64(3):177–86.
[53] Singh R, Mal G, Kumar D, Patil NV, Pathak KML. Camel milk: an important natural adjuvant. Agric Res 2017;6(4):327–40.